Metrol. Meas. Syst., Vol. 32 (2025) No. 3, pp. 1–18
DOI: 10.24425/mms.2023.155803

PAN POLSKA AKADEMIA NAUK

METROLOGY AND MEASUREMENT SYSTEMS
Index 330930, ISSN 0860-8229
www.metrology.wat.edu.pl

M&MS

FREQUENCY STABILITY OF SOFTWARE-DEFINED RADIOS – PART I. MEASUREMENTS

Kacper Bednarz[1)], Jarosław Wojtuń[1)], Jan M. Kelner[1)], Cezary Ziółkowski[1)], Czesław Leśnik[2)]

1) Military University of Technology, Faculty of Electronics, Institute of Communications Systems, ul. gen. Sylwestra Kaliskiego 2, 00-908 Warsaw (✉ *jaroslaw.wojtun@wat.edu.pl*)
2) Military University of Technology, Faculty of Electronics, Institute of Radioelectronics, ul. gen. Sylwestra Kaliskiego 2, 00-908 Warsaw

Abstract

The popularity and high efficiency of the software-defined radio (SDR) architecture led to its export to other areas of technology, *e.g.*, software-defined networks, vehicles, infrastructure, *etc.* These devices, as commercials off-the-shelfs (COTS), are the basis for numerous implementations and prototyping of new solutions. SDR allows for easy adoption of existing or development and testing of new communication standards, protocols, etc., also thanks to the support of open and free applications. SDR frequency stability is important in numerous applications, especially in techniques based on frequency measurement. This paper presents the methodology for frequency stability measurements for several popular COTS SDR platforms. Measurement was conducted in two variants, with and without an external rubidium frequency standard (RFS). We generally analyse two groups of frequency stability metrics, *i.e.*, the fundamental parameters and the Allan deviation that provide a comparison of measurement and manufacturer datasheet. These parameters are analysed as a function of time depending on the selected measurement intervals. We determine the distribution of the parameters tested, which is the basis for assessing and classifying SDRs. The results obtained can serve as a basis for modelling the SDR instability phenomenon in future simulation studies, including our own planned work as well as broader research conducted by the scientific community.

Keywords: software-defined radio (SDR), frequency stability, Allan deviation, measurement, modelling.

1. Introduction

Traditional radio communication systems are usually designed for a specific application, which can lead to limitations in flexibility and reconfigurability. The development of *software-defined radios* (SDR) introduces new possibilities for the design of communication systems, both in terms of flexibility and efficiency [1, 2]. It is crucial to continuously monitor technological progress to adapt to the dynamically changing communication environment. Software-defined radio is constantly evolving, driving innovation in wireless communications [3, 4].

Article history: April 7, 2025; revised July 8, 2025; accepted August 13, 2025; available online September 17, 2025.

SDR technology has been used for many years in the consumer, commercial, and military sectors. In addition to the previously mentioned reconfigurability, SDRs consume much less energy than traditional radios, which makes them much more efficient, thus enabling implementation in battery-powered devices, *e.g.* sensors and mobile phones. Thanks to the use of digital signal processing, SDR technology also enables the implementation of much more advanced signal processing functions, which mainly affect the quality of the received signals. Therefore, it can be said that SDR is the future of radio technology [4, 5]. Hence, it is impossible to list all its directions of SDR development. The first is the integration of *artificial intelligence* (AI) algorithms, especially *machine learning* (ML), [4, 6, 7]. Using AI algorithms, it is possible to automatically adapt both the modulation and the waveform used to the conditions that prevail in the communication channel [8, 9]. Integration with subsequent generations of mobile network standards, such as *Long Term Evolution* (LTE), *fifth generation New Radio* (5G NR), or *six generation* (6G), is also an important element of the development of SDR. This technology also plays a key role in ensuring reliable vehicle connectivity [10, 11].

SDR is also being developed on the military market [12]. Today, it is difficult to find new radios that are not based on this technology [13]. Thanks to a wide range of operating frequencies, spectrum monitoring and quick tuning, it allows us to carry out electromagnetic attacks and to protect against them. Minimising the size of the SDR means that it is increasingly used in implementations in *unmanned aerial vehicles* (UAVs) [14, 15], allowing the development of new technologies related to identifying and locating enemy forces [16]. Additionally, in the case of Doppler effect-based localisation methods [16, 17], frequency stability is crucial for localisation accuracy in contrast to other methods, *e.g.* [18].

Frequency stability is a frequently discussed topic in metrology journals [19–21]. Many SDR-based sensor applications require high frequency stability. For this reason, the paper focuses on the methodology of measurement for selected *commercial off-the-shelf* (COTS) SDR platforms. The presented analysis is based on the results of frequency stability measurements of SDR platforms made without or using a *rubidium frequency standard* (RFS). The study was performed with an additional external frequency standard to assess how it will affect the frequency stability of the SDRs. The results obtained will facilitate decision making in future sensor implementations as to whether their use is necessary. In the SDR datasheets, frequency accuracy is often omitted or given based only on the accuracy of the oscillator used in an SDR platform. The method and range of empirically determining the frequency accuracy, and on this basis classification of SDR, constitute the originality and novelty of this paper.

This paper consists of two parts. The main contributions of Part I are listed below.

- SDR platforms are described with particular emphasis on frequency accuracy, weight, size, and power consumption.
- The methodology for frequency stability measurements for SDR platforms is presented.
- Based on empirical studies, SDR platforms in terms of frequency stability are classified.
- The effectiveness of using RFS to minimise the frequency instability error of the local SDR generator is demonstrated.

The main aim of this paper is to develop and present a methodology for empirical evaluation of frequency stability in selected commercial SDR platforms, with and without the use of an RFS.

Part II of this paper [22] focuses on the use of measurement results to model the SDR frequency instability phenomenon for simulation studies.

The remainder of the paper is organised as follows. Section 2 briefly discusses the SDR platforms. Section 3 shows the testbed and measurement methodology. Section 4 includes the results of the measurement of the frequency stability of SDR platforms. The synthesis of the results is also presented, which allowed us to compare the SDR platforms. Section 6 provides a summary.

2. Comparison of SDR Platforms

For the research, it was decided to choose SDRs that are widely available on the market. Moreover, they are often used in various sensor implementations requiring high frequency stability. However, they come from different price ranges and, therefore, are characterised by different stability parameters (Tab. 1).

The first of them, ADALM-PLUTO, is an educational platform that by default operates in the frequency range from 325 to 3800 MHz. It is possible to extend this range through a software modification, which allows the radio to operate from 70 to 6000 MHz [23]. The SDR has one transmitting and one receiving *SubMiniature version A* (SMA) output. The frequency accuracy declared by the manufacturer of ADALM-PLUTO is ±25 ppm [24].

An even smaller and lighter solution is the *Universal Software Radio Peripheral* (USRP) B200mini equipped with the highly integrated *radio frequency* (RF) Agile Transceiver AD9364 [25]. It enables transmitting and receiving in the range of 70–6000 MHz with a bandwidth of 56 MHz. The frequency accuracy specified in the device specifications is ±2 ppm.

Another compact and very interesting solution is the bladeRF 2.0 micro xA4 from Nuand [26]. The radio frequency range is 47–6000 MHz for receiving and 70–6000 MHz for transmitting with a maximum bandwidth of 56 MHz. Using a *global positioning system disciplined oscillator* (GPSDO) in laboratory tests, a 1 GHz carrier can be accurate to approximately 500 mHz (±0.5 ppb).

The USRP N210 from the networked series [27] is much larger than its predecessors. The platform was tested with three different daughterboards: WBX, RFX1200, and XCVR2450. The operating frequency ranges are as follows: 50–2200 MHz for WBX, 1150–1450 MHz for RFX1200, 2400–2500 MHz and 4900–5900 MHz for XCVR2450 [28]. The frequency accuracy of the SDR is estimated to be ±2.5 ppm.

The USRP-2930 is another SDR included in our tests. The operating frequency range of the platform is 50–2200 MHz with a maximum instantaneous real-time bandwidth of 40 MHz. The frequency accuracy of the implemented *oven-controlled crystal oscillator* (OCXO) is equal to ±25 ppb if not connected to the *global positioning system* (GPS) and ±10 ppb if connected to GPS [29].

Table 1. Selected technical parameters of the tested platforms.

SDR Platform	Frequency Range (MHz)	Max Bandwidth (MHz)	Frequency Accuracy (ppm)	Power Consumption (W)	Dimensions (mm)**	Weight (g)
ADALM-PLUTO	70–6000	20	±25	2.5	78 × 117 × 23	116
B200mini	70–6000	56	±2	2.5	55 × 79 × 16	108
bladeRF 2.0 micro xA4	47(70)–6000*	56	±0.026	4.5	72 × 110 × 24	112
N210 + WBX	70–6000	40	±2.5	13.8	160 × 204 × 48	1160
N210 + XCVR2450	2400–2500 & 4900–5900	48	±0.025	12–15	160 × 204 × 48	1218
N210 + RFX1200	1150–1450	40	±0.025	12–15	160 × 204 × 48	1218
NI-2930	50–2200	40	±0.025	38–44	218 × 267 × 39	1787
NI-2950R	50–2200	120	±0.025	38–44	218 × 267 × 39	1787

*For bladeRF 2.0 micro xA4, the frequency ranges are 47–6000 MHz or 70–6000 MHz for Tx and Rx, respectively. **width × depth × height.

The most expensive SDR we tested is the USRP-2950R. Its frequency accuracy is the same as that of USRP-2930, which corresponds to ±25 ppb. When connected to GPS, its frequency accuracy can reach even ±5 ppb. The operating frequency range is also identical to its predecessor, however, the USRP-2950R operating instantaneous real-time bandwidth is up to 120 MHz [30].

A comparison of the frequency parameters, power consumption, dimensions, and weights of tested SDRs is presented in Table 1.

3. Measurement Testbed and Methodology

3.1. Testbed

The block scheme of the testbed for measuring the frequency stability of SDR platforms is shown in Fig. 1. A photo of the actual testbed assembled in the laboratory is shown in Fig. 2.

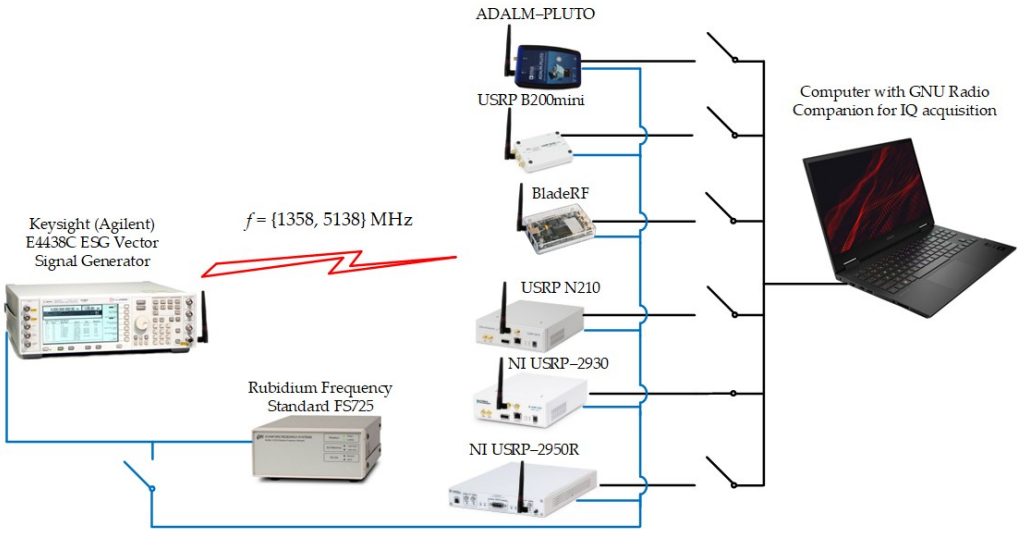

Fig. 1. Block scheme of the testbed for frequency stability measurement.

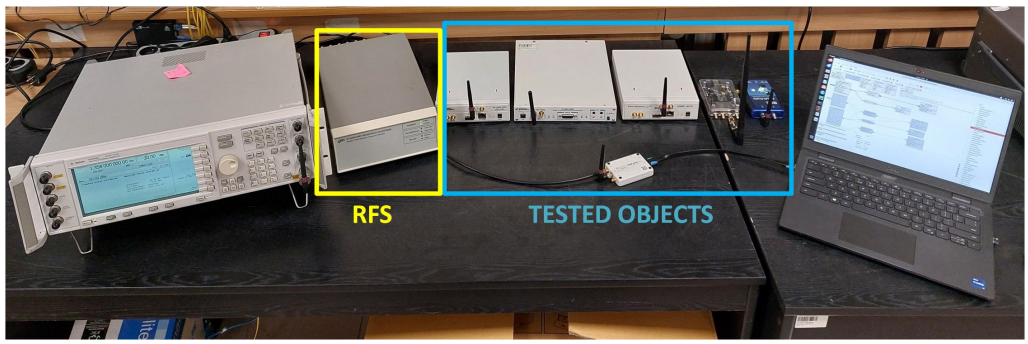

Fig. 2. Actual testbed for frequency stability measurement assembled in the laboratory.

The testbed consists of a transmitting part and a receiving part. The transmission part includes a Keysight (Agilent) E4438C ESG Vector Signal Generator with an attached FS725 RFS. The receiving part includes a laptop for recording, analysing and processing signals, as well as the SDR platforms described in the previous chapter.

The study was carried out in two variants: the first variant assumed no stabilisation of SDR platforms with a frequency standard, while in the second variant the platforms were stabilised. *The GNU Radio Companion* (GRC) environment, visible on the laptop screen in Fig. 2, was used to record the signal. The GRC environment allows for the simple connection of various SDRs and recording of signals without the need to write complex software, which is why it was decided to use it. Further analysis and signal processing were performed in the MATLAB environment, which allows for a more advanced visualisation of the research results. One SDR was tested at a time. It was decided to perform the test for two significantly different frequencies $f = 1358$ MHz and $f = 5138$ MHz.

All SDRs were tested at frequency $f = 1358$ MHz: ADALM-PLUTO, USRP B200mini, bladeRF 2.0 micro xA4, USRP N210 with the WBX or RFX1200 daughterboard, USRP-2930, USRP-2950R. At frequency $f = 5138$ MHz only three SDRs were tested: USRP B200mini, bladeRF 2.0 micro xA4, USRP N210 with XCVR2450 daughterboard.

During the measurements, a complex harmonic signal was generated from the Keysight (Agilent) E4438C ESG Vector Signal Generator shown in Fig. 1 and Fig. 2, at the carrier frequency $f_0 = f + 10$ kHz. This signal was received on SDRs using the GNU Radio Companion environment. The receiver frequency was equal to the test frequency f.

3.2. Methodology

De-tuning between Rx and Tx is done to minimise the effect of the DC component, which occurs when a quadrature signal is processed in the baseband. Ideally, after shifting the spectrum to the baseband and taking the 10 kHz offset between the receiver frequency f and the carrier frequency f_0 of the transmitted signal into account, the instantaneous frequency measured in the baseband f_p of the received signal should be 0 Hz. In fact, we are dealing with instability imposed by the internal oscillator of the SDR or the external RFS FS725, so the frequency value of the received signal changes as a function of time.

The sampling frequency f_s of the received signal was set to almost the lowest possible for the SDR tested. For this reason, for the bladeRF 2.0 micro xA4 it was $f_s = 600$ kHz, while for the other SDRs it was $f_s = 200$ kHz. The signal was recorded for 45 minutes.

In MATLAB environment, the received signal $x(t)$ was further analysed in the frequency domain, and therefore the received samples were transformed using *fast Fourier transform* (FFT) algorithms. The number of samples transformed in a single iteration was equal to $t_A \cdot f_s$ where t_A is the acquisition time and f_s is the sampling frequency mentioned above, as shown in Fig. 3. The frequency resolution of the FFT was constant and equal to $\Delta f = 0.01$ Hz. Then, the maximum in the obtained spectrum was determined, and the corresponding frequency value f_p was assigned to the appropriate place on the time axis of the graph showing the changes in instantaneous frequency measured in the baseband f_p of the signal as a function of time, which is visible at the bottom of Fig. 3. Subsequently, the analysis window of the mentioned size $t_A \cdot f_s$ was shifted in the time domain of the $x(t)$ signal by the value Δt_A, and subsequent samples were subjected to identical calculations to determine the next value of the instantaneous frequency of the signal measured in baseband f_p. The basis for further consideration of the recorded results is statistical analysis [31], also considering the Allan deviation [32].

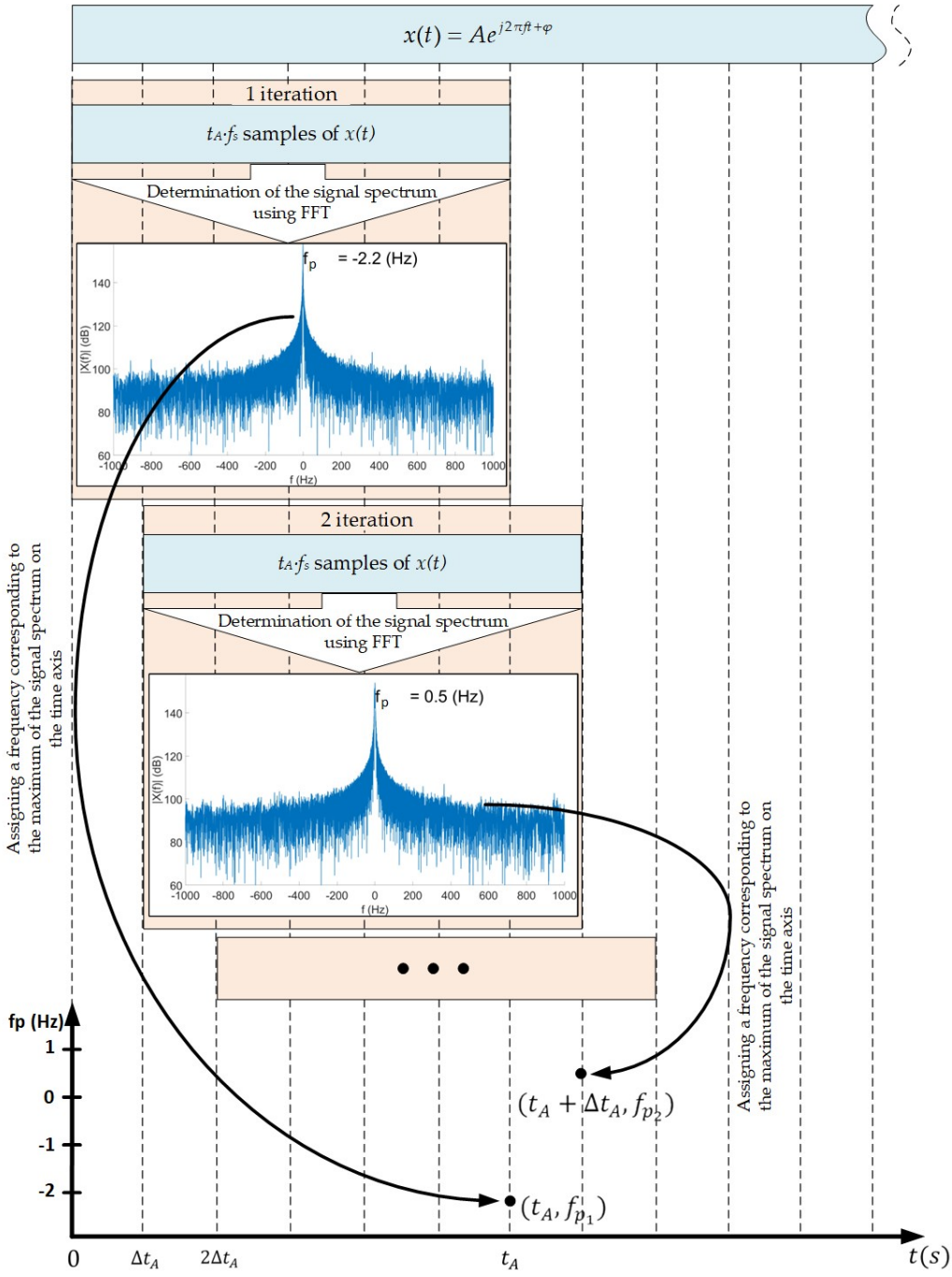

Fig. 3. Method for determining the plots of instantaneous frequency measured in baseband f_p of the received signal as a function of time using overlapping.

An example of instantaneous frequency measured in baseband f_p of the received signal as a function of time $f_p(t)$ is shown in Fig. 4.

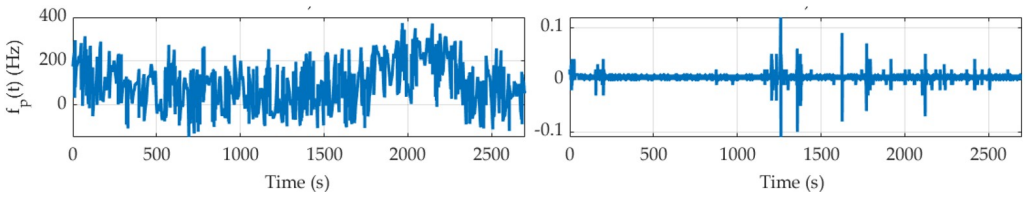

Fig. 4. Example of instantaneous frequency measured in baseband f_p versus time (f = 1358 MHz, t_A = 1 s, Δt_A = 0.1 s) without RFS on the left and with RFS on the right for USRP-2930.

4. Measurement Results

4.1. Calculation of Fundamental Metrics

The following fundamental metrics and equations that describe them were used to assess the frequency stability of the SDRs studied:

1. Mean value of instantaneous frequency measured in baseband μ_f:

$$\mu_f = \frac{1}{K}\sum_{k=1}^{K} f_{pk}, \tag{1}$$

where $k = 1, 2, \ldots, K$ is the index of the selected measurement and K is the number of all measurement values.

2. Frequency oscillation range O_R:

$$O_R = f_{p\max} - f_{p\min}, \tag{2}$$

where $f_{p\max}$ and $f_{p\min}$ are the maximum and minimum of the instantaneous frequency measured in the baseband, respectively.

3. Standard deviation of instantaneous frequency measured in the baseband σ_f:

$$\sigma_f = \sqrt{\frac{1}{K-1}\sum_{k=1}^{K}\left|f_{pk} - \mu_f\right|^2}. \tag{3}$$

4. Frequency stability s_f [33–35]:

$$s_f = \frac{\sigma_f}{f_0}, \tag{4}$$

where f_0 means the carrier frequency of the signal generated.

In the next step of assessing the frequency stability of selected COTS SDRs, we analyse the values of these parameters. The calculated metrics for t_A = 1 s, Δt_A = 0.1 s, at the two carrier frequencies tested are presented in Table 2 for the first carrier frequency (f = 1358 MHz) and in Table 3 for the second carrier frequency (f = 5138 MHz).

The values of the measured parameters differ by up to several orders of magnitude. For example, for 1358 MHz, without the clock synchronization signal, mean instantaneous frequency is from 10^1 Hz (for bladeRF 2.0) to 10^4 Hz (for ADALM-PLUTO), standard deviation of instantaneous

frequency is from 10^0 Hz (for B200mini) to 10^2 Hz (for ADALM-PLUTO and N210 + WBX), frequency stability is in the order of 10^{-9} (for B200mini) to 10^{-7} (for ADALM-PLUTO and N210 + WBX), and oscillation range is in the order from 10^1 Hz (for B200mini) to 10^3 Hz (for ADALM-PLUTO and N210 + WBX). When using an external frequency standard for 1358 MHz, the mean instantaneous frequency is from 10^{-3} Hz (for N210 + WBX and NI-2930) to 10^1 Hz (for ADALM-PLUTO), the standard deviation of instantaneous frequency is from 10^{-3} Hz (for N210 + RFX1200) to 10^0–10^1 Hz (for ADALM-PLUTO), frequency stability ranges from 10^{-12} Hz (for N210 + RFX1200) to 10^{-9} Hz (for ADALM-PLUTO), and oscillation range is from 10^{-1} Hz (for N210 + RFX1200) to 10^1 Hz (for ADALM-PLUTO).

Table 2. Frequency stability results for various SDR platforms (f = 1358 MHz, t_A = 1 s, Δt_A = 0.1 s).

SDR Platform	Without RFS				With RFS			
	μ_f (Hz)	σ_f (Hz)	s_f (–)	O_R (Hz)	μ_f (Hz)	σ_f (Hz)	s_f (–)	O_R (Hz)
ADALM-PLUTO	$1.67 \cdot 10^4$	$2.86 \cdot 10^2$	$2.11 \cdot 10^{-7}$	$1.19 \cdot 10^3$	$-5.50 \cdot 10^1$	$5.17 \cdot 10^0$	$3.81 \cdot 10^{-9}$	$3.89 \cdot 10^1$
B200mini	$1.44 \cdot 10^3$	$5.41 \cdot 10^0$	$3.98 \cdot 10^{-9}$	$3.72 \cdot 10^1$	$0.00 \cdot 10^0$	$1.30 \cdot 10^0$	$9.57 \cdot 10^{-10}$	$1.91 \cdot 10^1$
bladeRF	$-3.61 \cdot 10^1$	$3.52 \cdot 10^1$	$2.59 \cdot 10^{-8}$	$1.38 \cdot 10^2$	$-2.40 \cdot 10^{-1}$	$4.00 \cdot 10^{-3}$	$3.26 \cdot 10^{-12}$	$1.80 \cdot 10^{-1}$
N210 + WBX	$1.01 \cdot 10^3$	$1.85 \cdot 10^2$	$1.36 \cdot 10^{-7}$	$1.16 \cdot 10^3$	$4.00 \cdot 10^{-3}$	$1.40 \cdot 10^{-2}$	$1.05 \cdot 10^{-11}$	$8.00 \cdot 10^{-1}$
N210 + RFX1200	$1.18 \cdot 10^3$	$7.91 \cdot 10^1$	$5.82 \cdot 10^{-8}$	$4.17 \cdot 10^2$	$1.00 \cdot 10^{-2}$	$1.00 \cdot 10^{-3}$	$1.00 \cdot 10^{-12}$	$5.00 \cdot 10^{-2}$
NI-2930	$9.12 \cdot 10^1$	$9.76 \cdot 10^1$	$7.19 \cdot 10^{-8}$	$5.22 \cdot 10^2$	$4.00 \cdot 10^{-3}$	$7.00 \cdot 10^{-3}$	$5.04 \cdot 10^{-12}$	$2.30 \cdot 10^{-1}$
NI-2950R	$9.28 \cdot 10^2$	$1.41 \cdot 10^1$	$1.04 \cdot 10^{-8}$	$7.07 \cdot 10^1$	$-2.00 \cdot 10^{-2}$	$3.00 \cdot 10^{-3}$	$1.89 \cdot 10^{-12}$	$9.00 \cdot 10^{-2}$

Table 3. Frequency stability results for various SDR platforms (f = 5138 MHz, t_A = 1 sΔt_A = 0.1 s).

SDR Platform	Without RFS				With RFS			
	μ_f(Hz)	σ_f (Hz)	s_f (–)	O_R (Hz)	μ_f (Hz)	σ_f (Hz)	s_f (–)	O_R (Hz)
B200mini	$5.52 \cdot 10^3$	$7.16 \cdot 10^1$	$1.39 \cdot 10^{-8}$	$2.82 \cdot 10^2$	$-2.00 \cdot 10^{-3}$	$5.22 \cdot 10^0$	$1.02 \cdot 10^{-9}$	$1.15 \cdot 10^2$
bladeRF	$5.52 \cdot 10^2$	$9.55 \cdot 10^2$	$1.86 \cdot 10^{-7}$	$2.45 \cdot 10^3$	$-1.67 \cdot 10^0$	$5.00 \cdot 10^{-3}$	$9.46 \cdot 10^{-13}$	$9.00 \cdot 10^{-2}$
N210 + XCVR2450	$4.73 \cdot 10^3$	$3.73 \cdot 10^2$	$7.26 \cdot 10^{-8}$	$2.09 \cdot 10^3$	$1.10 \cdot 10^{-2}$	$5.00 \cdot 10^{-3}$	$9.95 \cdot 10^{-13}$	$8.00 \cdot 10^{-2}$

Based on the results of the measurements, it can be seen that the use of an external clock generally improves the stabilisation parameters of the COTS platforms by 2–4 orders of magnitude. Considering the results obtained, it can be concluded that ADALM-PLUTO is characterised by the worst clock stabilisation parameters. The use of a frequency standard does not significantly improve the parameters of this platform. Therefore, we do not recommend using this SDR in applications where clock synchronisation and stability play a crucial role. B200mini has the best parameters without an external clock, while connecting the frequency standard improves its metrics, but in this case this SDR is not classified at the top of the list. The best parameters using the frequency standard were obtained for the N210 + RFX1200, while the N210 + WBX platform without a clock had some of the worst parameters.

Operation in higher frequency ranges is only possible for three platforms, which are characterised by relatively good parameters with and without an external clock. Hence, considering all these aspects, we recommend the use of B200mini and bladeRF 2.0 as the best platforms operating in a wide frequency range with and without an external frequency reference, respectively. The small size and weight are their additional advantage, which allows implementing these COTS SDRs in UAVs.

4.2. Comparison of Manufacturer Data and Measurement Results

The frequency stability in a crystal oscillator is usually represented in relative units, the so-called ppm. The conversion of the ppm value to the equivalent frequency accuracy in Hz is realised as follows:

$$\delta_f \text{ (Hz)} = \Delta F \text{ (ppm)} \cdot f_0 \text{ (MHz)} \tag{5}$$

where ΔF and f_0 means the frequency accuracy and carrier frequency of the generated signal, respectively.

The frequency stability results based on manufacturer data and measurements for analysed COTS SDRs are presented in Table 4 and Table 5 for 1358 MHz and 5138 MHz, respectively.

Table 4. Comparison of tested SDR platforms based on manufacturer and measurement results for f = 1358 MHz.

SDR Platform without External Oscillator	**Manufacturer Data**		**Measurement Data, t_A = 1 s, Δt_A = 0.1 s**	
	ΔF (ppm)	δ_f (Hz)	μ_f (Hz)	σ_f (Hz)
ADALM-PLUTO	±25	$3.39 \cdot 10^4$	$1.67 \cdot 10^4$	$2.86 \cdot 10^2$
N210 + WBX	±2.5	$3.39 \cdot 10^3$	$1.01 \cdot 10^3$	$1.85 \cdot 10^2$
N210 + RFX1200	±2.5	$3.39 \cdot 10^3$	$1.18 \cdot 10^3$	$7.91 \cdot 10^1$
B200mini	±2	$2.72 \cdot 10^3$	$1.44 \cdot 10^3$	$5.41 \cdot 10^0$
bladeRF 2.0 micro xA4	±0.026	$3.40 \cdot 10^1$	$-3.61 \cdot 10^1$	$3.52 \cdot 10^1$
NI–2950R	±0.025	$3.39 \cdot 10^1$	$9.28 \cdot 10^2$	$1.41 \cdot 10^1$
NI–2930	±0.025	$3.39 \cdot 10^1$	$9.12 \cdot 10^1$	$9.76 \cdot 10^1$
SDR Platform with External Oscillator	with GPSDO		with FS725 RFS	
ADALM-PLUTO	n/a	n/a	$-5.50 \cdot 10^1$	$5.17 \cdot 10^0$
N210 + WBX	±0.01	$1.36 \cdot 10^1$	$4.00 \cdot 10^{-3}$	$1.40 \cdot 10^{-2}$
N210 + RFX1200	±0.01	$1.36 \cdot 10^1$	$1.00 \cdot 10^{-2}$	$1.00 \cdot 10^{-3}$
B200mini	n/a	n/a	$0.00 \cdot 10^0$	$1.30 \cdot 10^0$
bladeRF 2.0 micro xA4	±0.0005	$6.79 \cdot 10^{-1}$	$-2.40 \cdot 10^{-1}$	$4.00 \cdot 10^{-3}$
NI–2950R	±0.005	$6.79 \cdot 10^0$	$-2.00 \cdot 10^{-2}$	$3.00 \cdot 10^{-3}$
NI–2930	±0.01	$1.36 \cdot 10^1$	$4.00 \cdot 10^{-3}$	$7.00 \cdot 10^{-3}$

Table 5. Comparison of tested SDR platforms based on manufacturer and measurement results for f =5138 MHz.

SDR Platform without External Oscillator	**Manufacturer Data**		**Measurement Data, t_A = 1 s, Δt_A = 0.1 s**	
	ΔF (ppm)	δ_f (Hz)	μ_f (Hz)	σ_f (Hz)
N210 + XCVR2450	±2.5	$1.28 \cdot 10^4$	$4.73 \cdot 10^3$	$3.73 \cdot 10^2$
B200mini	±2	$1.03 \cdot 10^4$	$5.52 \cdot 10^3$	$7.16 \cdot 10^1$
bladeRF 2.0 micro xA4	±0.026	$1.34 \cdot 10^2$	$5.52 \cdot 10^2$	$9.55 \cdot 10^2$
SDR Platform with External Oscillator	with GPSDO		with FS725 RFS	
N210 + XCVR2450	±0.01	$5.14 \cdot 10^1$	$1.10 \cdot 10^{-2}$	$5.00 \cdot 10^{-3}$
B200mini	n/a	n/a	$-2.00 \cdot 10^{-3}$	$5.22 \cdot 10^0$
bladeRF 2.0 micro xA4	±0.0005	$2.57 \cdot 10^0$	$-1.67 \cdot 10^0$	$5.00 \cdot 10^{-3}$

Comparing the frequency accuracy δ_f calculated according to formula (5) with the results of empirical studies for the case without RFS, we can see that the standard deviation σ_f calculated according to formula (3) is in most cases even several orders smaller than the frequency accuracy δ_f. To compare them, it is necessary to also include the mean value μ_f in the empirical results. The val-

ues obtained then are comparable. However, the results of studies with RFS are difficult to compare because the manufacturers provide data only for stabilisation with GPSDO. Much better results were obtained in this case for empirical studies with RFS, for which σ_f could reach values on the order of a few millihertz ($i.e.$, 10^{-3} Hz), while the frequency accuracy δ_f was of the order of single hertz.

4.3. Influence of data acquisition time on instantaneous frequency estimation

The example graph presented in Fig. 4 was obtained for an acquisition time equal to 1 s. The influence of changes in this parameter on the analysed frequency stability phenomenon was shown using the example of the selected SDR. For this purpose, we had chosen the bladeRF 2.0 platform, which from the point of view of the application presented in [17, 35] provides sufficient stability with and without an external frequency standard in terms of the frequency oscillation range. For this SDR, we also show plots of instantaneous frequency versus time in Fig. 5 for 1358 MHz and different acquisition times, $t_A = [0.1, 1, 10, 100]$ s.

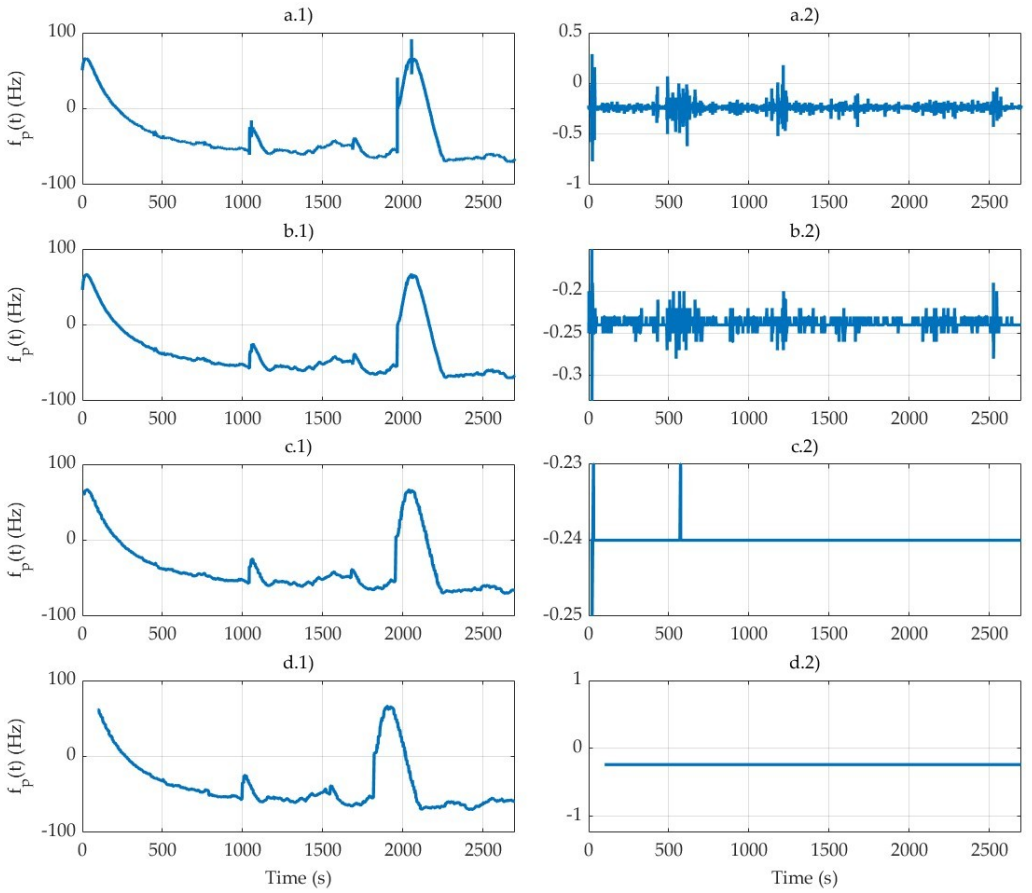

Fig. 5. Exemplary bladeRF's plots of instantaneous frequency measured in baseband f_p versus time without RFS on the left and with RFS on the right for $f = 1358$ MHz, $\Delta t_A = 0.1$ s, and different acquisition time: a) $t_A = 0.1$ s, b) $t_A = 1$ s, c) $t_A = 10$ s, d) $t_A = 100$ s.

Regardless of the adopted acquisition time, the nature of changes in the instantaneous frequency is generally the same. This is especially noticeable in cases without a frequency standard (see the graph on the left of Fig. 5). The use of a stable external clock allows one to eliminate the trend of changes in average instantaneous frequency (see plot to the right of Fig. 5). In this case, increasing the acquisition time allows further reduction of frequency fluctuations of the obtained plots. For $t_A = 100$ s, the instantaneous frequency of the received signal is fully stabilised on the obtained plot and does not have any oscillations. In some graphs, we can see frequency jumps resulting from operation of atomic clocks, which is also mentioned in [21].

5. Allan Deviation

The measure of frequency stability used to assess the stochastic stability of a clock as a function of the averaging time (measurement interval τ) is the Allan deviation σ_{Af}, expressed by the following formula [32, 36]:

$$\sigma_{Af}(\tau) = \sqrt{\frac{1}{2(K-1)} \sum_{k=1}^{K-1} \left(f_p^{k+1} - f_p^k\right)^2}, \tag{6}$$

where f_p^k is the frequency difference between the measured frequency and the nominal frequency (in our case, this is the previously determined value of instantaneous frequency measured in the baseband f_p) averaged over the measurement interval τ [37]:

$$f_p^k = \frac{1}{\tau} \int_{t_k}^{t_k+\tau} f_p(t)\mathrm{d}t, \tag{7}$$

and K is the number of all averaged frequencies f_p^k.

We paid special attention to Allan deviation measurements, as a standardized frequency stability metric widely used by equipment manufacturers and research centres [34, 38, 39]. Exemplary Allan deviation plots versus averaging time obtained during measurements for tested SDRs are shown in Fig. 6 and Fig. 7 for 1358 MHz and 5138 MHz, respectively.

The obtained results show that the conclusions from the Allan deviation analysis coincide in key issues obtained with the analysis of other parameters presented in Sections 4.1 and 4.2. The graphs clearly illustrate how an external frequency standard significantly improves the stability of the SDRs clock. The Allan deviation plots for the SDR study with the external clock attached are several orders of magnitude lower than those for the SDR without it. In this case, the exceptions are ADALM-PLUTO (for 1358 MHz) and B200mini (for 1358 MHz and 5138 MHz), for which the Allan deviation measured with the external clock attached achieves values that are comparable to those obtained for the other SDRs tested without the external frequency clock attached. It is also interesting that for ADALM-PLUTO the Allan deviation measured without an external clock connected to the SDR is better (*i.e.* smaller) for the averaging time $\tau \leq 2$ s than for the test conducted with an external clock connected to the SDR. Similarly, for B200mini the Allan deviation measured without an external clock connected to the SDR is better for the averaging time $\tau \leq 8$ s (for 1358 MHz) and $\tau \leq 5$ s (for 5138 MHz) than for the test conducted with an external clock connected to the SDR.

The acquisition time t_A in the provided examples is 1 s with Δt_A step 0.1 s. A summary of Allan deviation results for various acquisition times t_A and a single averaging time $\tau = 1$ s is presented in Table 6 and Table 7 for $f = 1358$ MHz and $f = 5138$ MHz, respectively.

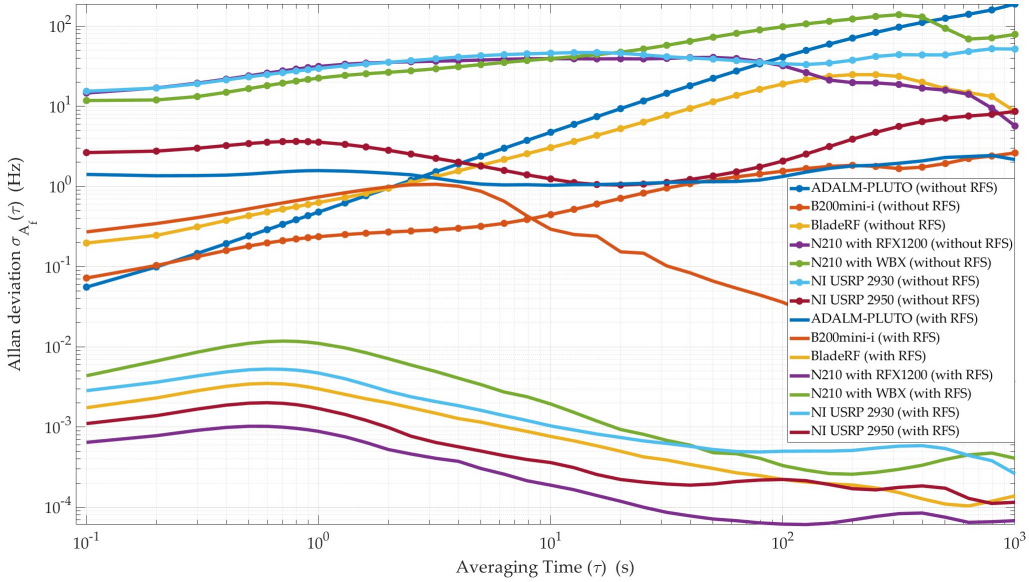

Fig. 6. Allan deviation versus averaging time for COTS SDRs and $f = 1358$ MHz.

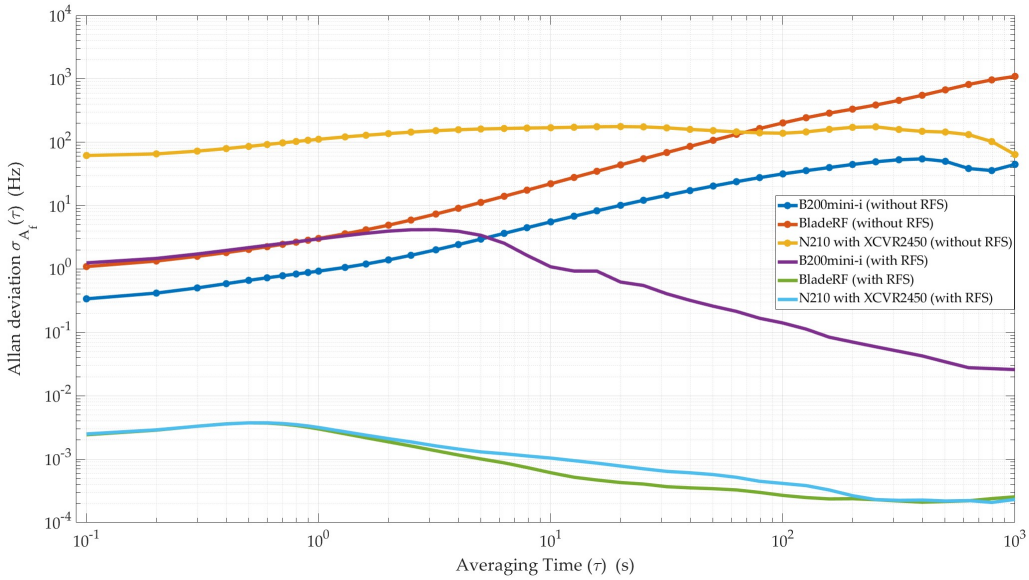

Fig. 7. Allan deviation versus averaging time for COTS SDRs and $f = 5138$ MHz.

Based on Fig. 6 and Fig. 7, the Allan deviation takes values from 10^{-4} to 10^{2} which gives 6 orders of magnitude. The range of Allan deviation changes is even greater based on calculations for different acquisition times. Analysing Table 6 and Table 7, we can see that the Allan deviation changes range from about 10^{-10} to 10^{4}, which gives 14 orders of magnitude. Based on the plots presented in Fig. 6 and Fig. 7, the devices were classified according to the value of this parameter. Hence, we propose to set two blur limits at the levels 10^{-2} and 10^{0} Hz, which allow the tested

Table 6. Allan deviations for all tested SDRs, 1358 MHz and different acquisition time t_A.

t_A (s)	0.1	1	10	100	0.1	1	10	100
SDR Platform	**Without RFS**				**With RFS**			
	Allan Deviation (Hz)							
ADALM-PLUTO	$2.30 \cdot 10^{-1}$	$2.30 \cdot 10^{-1}$	$2.79 \cdot 10^{0}$	$2.47 \cdot 10^{0}$	$4.60 \cdot 10^{0}$	$2.49 \cdot 10^{0}$	$6.35 \cdot 10^{-1}$	$6.25 \cdot 10^{-1}$
B200mini	$6.90 \cdot 10^{-2}$	$5.60 \cdot 10^{-2}$	$1.80 \cdot 10^{-2}$	$1.80 \cdot 10^{-2}$	$5.53 \cdot 10^{-1}$	$5.49 \cdot 10^{-1}$	$1.79 \cdot 10^{-1}$	$1.80 \cdot 10^{-1}$
bladeRF 2.0 micro xA4	$4.69 \cdot 10^{-1}$	$3.97 \cdot 10^{-1}$	$7.01 \cdot 10^{-1}$	$7.30 \cdot 10^{-1}$	$2.42 \cdot 10^{-5}$	$8.96 \cdot 10^{-6}$	$7.31 \cdot 10^{-8}$	$<10^{-10}$
N210 + RFX1200	$1.03 \cdot 10^{3}$	$9.84 \cdot 10^{2}$	$3.59 \cdot 10^{2}$	$3.64 \cdot 10^{2}$	$5.12 \cdot 10^{-5}$	$7.81 \cdot 10^{-7}$	$<10^{-10}$	$<10^{-10}$
N210 + WBX	$5.08 \cdot 10^{2}$	$5.04 \cdot 10^{2}$	$4.52 \cdot 10^{2}$	$4.45 \cdot 10^{2}$	$2.51 \cdot 10^{-4}$	$1.22 \cdot 10^{-4}$	$2.04 \cdot 10^{-6}$	$1.60 \cdot 10^{-7}$
NI–2930	$9.02 \cdot 10^{3}$	$8.76 \cdot 10^{2}$	$4.72 \cdot 10^{2}$	$4.82 \cdot 10^{2}$	$3.58 \cdot 10^{-5}$	$2.22 \cdot 10^{-5}$	$1.93 \cdot 10^{-6}$	$9.03 \cdot 10^{-8}$
NI–2950R	$1.40 \cdot 10^{1}$	$1.27 \cdot 10^{1}$	$2.53 \cdot 10^{0}$	$2.58 \cdot 10^{0}$	$1.83 \cdot 10^{-5}$	$2.90 \cdot 10^{-6}$	$<10^{-10}$	$<10^{-10}$

Table 7. Allan deviations for all tested SDRs, 5138 MHz and different acquisition time t_A.

t_A (s)	0.1	1	10	100	0.1	1	10	100
SDR Platform	**Without RFS**				**With RFS**			
	Allan Deviation (Hz)							
B200mini	$9.78 \cdot 10^{-1}$	$8.57 \cdot 10^{-1}$	$1.41 \cdot 10^{0}$	$1.41 \cdot 10^{0}$	$8.79 \cdot 10^{0}$	$8.88 \cdot 10^{0}$	$2.87 \cdot 10^{0}$	$2.81 \cdot 10^{0}$
bladeRF 2.0 micro xA4	$9.18 \cdot 10^{0}$	$9.21 \cdot 10^{0}$	$2.28 \cdot 10^{1}$	$1.59 \cdot 10^{2}$	$5.12 \cdot 10^{-5}$	$8.98 \cdot 10^{-6}$	$2.49 \cdot 10^{-8}$	$<10^{-10}$
N210 + XCVR2450	$1.30 \cdot 10^{4}$	$1.24 \cdot 10^{4}$	$6.12 \cdot 10^{3}$	$6.14 \cdot 10^{3}$	$7.56 \cdot 10^{-5}$	$9.98 \cdot 10^{-6}$	$3.74 \cdot 10^{-8}$	$<10^{-10}$

SDRs to be divided into three classes in terms of clock stability. It was assumed that the first class of low-stability devices have Alan deviation values above 10^0 Hz. The second class of medium-stability devices has values ranging from 10^0 to 10^{-2} Hz. Devices for which the Allan deviation values are lower than 10^{-2} Hz were classified as third class devices with high-stability.

Based on this classification proposal and considering the Allan deviation for $f = 1358$ MHz and $\tau = 1$ s, N210 + RFX1200, N210 + WBX, NI–2930, and NI-2950R without RFS and ADALM-PLUTO with RFS are classified as low-stability class devices, ADALM-PLUTO, B200mini, and bladeRF 2.0 micro xA4 without RFS, and B200mini with RFS can be classified to medium-stability class devices, and bladeRF 2.0 micro xA4, N210 + RFX1200, N210 + WBX, NI-2930, and NI–2950R with RFS can be classified as high-stability class devices. Analogously, considering the Allan deviation for $f = 5138$ MHz and $\tau = 1$ s, N210 + XCVR2450 and bladeRF 2.0 micro xA4 without RFS and B200mini with RFS are classified as low-stability class devices, B200mini without RFS is classified as a medium-stability class device, and N210 + XCVR2450 and bladeRF 2.0 micro xA4 with RFS are classified as high-stability class devices.

6. Conclusions

This paper focuses on the measurement methodology, obtained result analysis, comparison of COTS SDR platforms regarding frequency stability. In our tests, we included six SDRs from three manufacturers, that is, ADALM-PLUTO, bladeRF 2.0 micro xA4, and four USRP models: B200mini, NI-2950R, NI-2930, and N210 with three daughterboards, WBX, RFX1200, and XCVR2450. Measurements were carried out for the 1358 and 5138 MHz frequencies and two variants, *i.e.*, without and with an external RFS. In the analysis, we used several metrics that allow

for evaluating the tested devices in terms of frequency stability. Based on the Allan deviation, we proposed dividing SDRs into three classes: low-, medium- and high-stability devices. We also compared the measurement results obtained with the data presented by the device manufacturers.

The frequency stability of transmitting and receiving devices (including radio devices) plays a crucial role in all telecommunications and navigation systems, particularly in synchronization processes and many applications, for example [38, 40]. From the point of view of using COTS SDR in potential UAV-based mobile applications, weight, size, and power consumption issues play the crucial role in addition to frequency stability.

The analysis and comparison presented provide essential information for potential SDR users or system designers about a critical feature of the devices for specific applications. The obtained results are the basis for modelling the effects of frequency instability in the design of devices that use SDRs. These issues are presented in the second part of this paper [22].

Acknowledgements

This work was developed within the framework of the research project on "Command and Control of Group of COMINT Radio-electronic Reconnaissance Unmanned Aerial Vehicles Based on Modern IT Technologies", with the acronym UAV-COMINT, no. DOB-SZAFIR/01/B/029/03/2021, sponsored by the National Centre for Research and Development (NCBR), Poland, under the Programme 3/SZAFIR/2021, and Grant no. UGB/22-059/2025/WAT, financed by the Military University of Technology (WAT), Poland.

References

[1] Goeller, L., & Tate, D. (2014). A technical review of software defined radios: vision, reality, and current status. In *2014 IEEE Military Communications Conference* (pp. 1466–1470). https://doi.org/10.1109/milcom.2014.242

[2] Ma*chado-Fern*ández, J.R. (2014). Software Defined Radio: Basic principles and applications. *Revista Facultad de Ingeniería*, *24*(38), 79. https://doi.org/10.19053/01211129.3160

[3] Krishnan, R., Babu, R.G., Kaviya, S., Kumar, N.P., Rahul, C., & Raman, S.S. (2017). Software defined radio (SDR) foundations, technology tradeoffs: A survey. *2017 IEEE International Conference on Power, Control, Signals and Instrumentation Engineering (ICPCSI)*, 2677–2682. https://doi.org/10.1109/icpcsi.2017.8392204

[4] Michailidis, E.T., Maliatsos, K., & Vouyioukas, D. (2024). Software-defined radio deployments in UAV-driven applications: A comprehensive review. *IEEE Open Journal of Vehicular Technology*, 1–43. https://doi.org/10.1109/ojvt.2024.3477937

[5] Hussain, W., Isoaho, J., & Nurmi, J. (2016). The Future of Software-Defined Radio: Recommendations. In *Springer eBooks* (pp. 237–238). https://doi.org/10.1007/978-3-319-49679-5_12

[6] Jdid, B., Hassan, K., Dayoub, I., Lim, W.H., & Mokayef, M. (2021). Machine Learning Based Automatic Modulation Recognition for Wireless Communications: A Comprehensive Survey. *IEEE Access*, *9*, 57851–57873. https://doi.org/10.1109/access.2021.3071801

[7] De La Rosa, J. M. (2022). AI-Assisted Sigma-Delta Converters – Application to Cognitive Radio. *IEEE Transactions on Circuits & Systems II: Express Briefs*, *69*(6), 2557–2563. https://doi.org/10.1109/tcsii.2022.3161717

[8] Skokowski, P., Malon, K., & Łopatka, J. (2022). Building the Electromagnetic Situation Awareness in MANET Cognitive Radio Networks for Urban Areas. *Sensors*, *22*(3), 716. https://doi.org/10.3390/s22030716

[9] Manco, J., Dayoub, I., Nafkha, A., Alibakhshikenari, M., & Thameur, H.B. (2022). Spectrum Sensing Using Software Defined Radio for Cognitive Radio Networks: A Survey. *IEEE Access*, *10*, 131887–131908. https://doi.org/10.1109/access.2022.3229739

[10] Lahoud, C., Ehsanfar, S., Gabriel, M., Kuffner, P., & Mosner, K. (2022). Experimental Testbed Results on LTE/5G-V2I Communication Using Software Defined Radio. *ICC 2022 – IEEE International Conference on Communications*, 2894–2899. https://doi.org/10.1109/icc45855.2022.9838411

[11] Zhang, J., Lu, K., Wan, Y., Xie, J., & Fu, S. (2024). Empowering UAV-Based Airborne Computing Platform with SDR: Building an LTE Base Station for Enhanced Aerial Connectivity. *IEEE Transactions on Vehicular Technology*, 1–14. https://doi.org/10.1109/tvt.2024.3406339

[12] Bergstrom, C., Chuprun, S., Gifford, S., & Maalouli, G. (2002). Software Defined Radio (SDR) Special Military Applications. In *Military Communications Conference MILCOM* (pp. 383–388). https://doi.org/10.1109/milcom.2002.1180472

[13] Mobile Experts LLC (2011) *Software Defined Radio (SDR): Market Shipments and Adoption Review*. Report Commissioned by Wireless Innovation Forum. Sep. 09, 2025. [Online]. Available: https://www.wirelessinnovation.org/assets/documents/mexp-sdr-11%20final.pdf

[14] Malatest B. (2023). Software defined radios (SDR) for electronic warfare. Apr. 24, 2023. [Online]. Available: https://www.everythingrf.com/community/software-defined-radios-sdr-for-electronic-warfare

[15] Rukaiya, R., Khan, S.A., Farooq, M.U., & Matloob, I. (2024). Communication architecture and operations for SDR-enabled UAVs network in disaster-stressed areas. *Ad Hoc Networks*, *160*, 103506. https://doi.org/10.1016/j.adhoc.2024.103506

[16] Szczepanik, R., & Kelner, J.M. (2025). Filtering and overlapping data for accuracy enhancement of Doppler-based location method. *Sensors*, *25*(5), 1465. https://doi.org/10.3390/s25051465

[17] Bednarz, K., Wojtuń, J., Kelner, J.M., & Różyc, K. (2024). Frequency Instability Impact of Low-Cost SDRs on Doppler-Based Localization Accuracy. *Sensors*, *24*(4), 1053. https://doi.org/10.3390/s24041053

[18] Matuszewski, J., & Kraszewski, T. (2021). Evaluation of emitter location accuracy with the modified triangulation method by means of maximum likelihood estimators. *Metrology and Measurement Systems*, *28*(4), 781–802. https://doi.org/10.24425/mms.2021.138537

[19] Mochizuki, K., Uchino, M., & Morikawa, T. (2007). Frequency-Stability measurement system using high-speed ADCs and digital signal processing. *IEEE Transactions on Instrumentation and Measurement*, *56*(5), 1887–1893. https://doi.org/10.1109/tim.2007.895588

[20] De La Rosa, J.J.G., Moreno, A., Lloret, I., Pallarés, V., & Liñán, M. (2006). Characterisation of frequency instability and frequency offset using instruments with incomplete data sheets. *Measurement*, *39*(7), 664–673. https://doi.org/10.1016/j.measurement.2006.01.001

[21] Marszalec, M., Lusawa, M., & Osuch, T. (2020b). Efficient frequency jumps detection algorithm for atomic clock comparisons. *Metrology and Measurement Systems*, 28(1), 107–121. https://doi.org/10.24425/mms.2021.135996

[22] Bednarz K., Wojtuń J., Kelner J.M., Ziółkowski C., & Leśnik C. (2025). Frequency stability of software-defined radios – Part II. Modelling for simulation studies. (in review), *Metrology and Measurement Systems*, *32*(4), 2025.

[23] "ADALM-PLUTO SDR hack: Tune 70 MHz to 6 GHz and GQRX install," rtl-sdr.com. Accessed: May 19, 2025. [Online]. Available: https://www.rtl-sdr.com/adalm-pluto-sdr-hack-tune-70-mhz-to-6-ghz-and-gqrx-install

[24] Analog Devices, "ADALM-PLUTO SDR active learning module." 2017. [Online]. Available: https://www.analog.com/media/en/news-marketing-collateral/product-highlight/adalm-pluto-product-highlight.pdf

[25] Ettus Research, "USRP B200mini-i." 2024. [Online]. Available: https://www.ettus.com/all-products/usrp-b200mini-i-2

[26] Nuand, "bladeRF 2.0 micro xA4." 2024. [Online]. Available: https://www.nuand.com/product/bladerf-xa4

[27] Ettus Research, "USRP networked series." 2024. [Online]. Available: https://www.ettus.com/product-categories/usrp-networked-series

[28] Ettus Research, "TX and RX daughterboards for the USRP software radio system," Olifantasia. [Online]. Available: https://www.olifantasia.com/gnuradio/usrp/files/datasheets/datasheet_daughterboards.pdf

[29] EMIN, "NI USRP-2930 USRP software defined radio device (50 MHz 2.2 GHz, 1-channel, GPSDO)." 2024. [Online]. Available: https://emin.com.mm/niusrp-2930781910-01-ni-usrp-2930-usrp-software-defined-radio-device-50-mhz-2-2-ghz-1-channel-gpsdo-100661/pr.html

[30] National Instruments, "USRP-2950 specifications." 2024. [Online]. Available: https://www.ni.com/docs/en-US/bundle/usrp-2950-specs/page/specs.html

[31] Przystupa, K., Kolodiy, Z., Yatsyshyn, S., Majewski, J., Khoma, Y., Petrovska, I., Lasarenko, S., & Hut, T. (2022). Standard deviation in the simulation of statistical measurements. *Metrology and Measurement Systems*, 30(1), 17–30. https://doi.org/10.24425/mms.2023.144403

[32] Greenhall, C., Howe, D., & Percival, D. (1999). Total variance, an estimator of long-term frequency stability [standards]. *IEEE Transactions on Ultrasonics Ferroelectrics and Frequency Control*, *46*(5), 1183–1191. https://doi.org/10.1109/58.796124

[33] Howe D.A. (1976). Frequency domain stability measurements: a tutorial introduction, *U.S. Department of Commerce, National Bureau of Standards, Institute for Basic Standards, Time and Frequency Division*, Washington, DC, NBS Technical Note 679, Mar. 1976. [Online]. Available: https://www.govinfo.gov/content/pkg/GOVPUB-C13-8becaeba7356ac60e56d89f36043ff7e/pdf/GOVPUB-C13-8becaeba7356ac60e56d89f36043ff7e.pdf

[34] Křen, P. (2012). Laser frequency counting and frequency modulation width measurement from an FFT signal. *Metrology and Measurement Systems*, *19*(3), 565–572. https://doi.org/10.2478/v10178-012-0049-0

[35] Kelner, J.M., Ziółkowski, C., & Marszałek, P. (2016). Influence of the frequency stability on the emitter position in SDF method. In *International Conference on Military Communications and Information Systems (ICMCIS)* (pp. 1–6). https://doi.org/10.1109/icmcis.2016.7496554

[36] Fernández, E., Calero, D., & Parés, M. (2017). CSAC characterization and its impact on GNSS clock augmentation performance. *Sensors*, *17*(2), 370. https://doi.org/10.3390/s17020370

[37] Dawkins, S.T., McFerran, J.J., & Luiten, A.N. (2007). Considerations on the measurement of the stability of oscillators with frequency counters. *IEEE Transactions on Ultrasonics Ferroelectrics and Frequency Control*, *54*(5), 918–925. https://doi.org/10.1109/tuffc.2007.337

[38] Gu, X., Zheng, C., Li, Z., Zhou, G., Zhou, H., & Zhao, L. (2023). Cooperative localization for UAV systems from the perspective of physical clock synchronization. *IEEE Journal on Selected Areas in Communications*, *42*(1), 21–33. https://doi.org/10.1109/jsac.2023.3322797

[39] Wang, G., Yao, Y., Yan, T., Bian, L., & Meng, Y. (2019). A new optical frequency transfer method via fibre based on active phase noise compensation with single acousto-optic modulator. *Metrology and Measurement Systems*, 26(1), 115–124. https://doi.org/10.24425/mms.2019.126334

[40] Berber, Z., Kameche, S., & Benkhelifa, E. (2019). High tolerance of charge pump leakage current in Integer-N PLL frequency synthesizer for 5G networks. *Simulation Modelling Practice and Theory*, *95*, 134–147. https://doi.org/10.1016/j.simpat.2019.04.010

Kacper Bednarz was born in Poland in 1997. He graduated from the Military University of Technology (WAT) in 2022 as the top student of the Faculty of Electronics, obtaining an M.Sc. degree in electronics and telecommunications. In 2023 he began his studies at the WAT Doctoral School. From 2022 he has worked works as an engineer at the Institute of Communication Systems, Faculty of Electronics, Military University of Technology. He is also a junior vice-chair of the F Commission on Wave Propagation and Remote Sensing of the Polish National Committee of the International Union of Radio Science – URSI. The scope of his scientific activity covers digital signal processing, wireless communications, the software-defined radio (SDR) technology, localization techniques, and sensing. As part of the Group of the Analysis, Modelling, and Estimation of Radio Channels (GAMERC), he is the contractor of four research projects on tactical radio reconnaissance from unmanned aerial vehicles (UAVs), command and management of a radio-electronic reconnaissance UAVs group, and long-range communications.

Jarosław Wojtuń received his B.Sc. and M.Sc. degrees in electronics and telecommunications and the Ph.D. in digital signal processing from the Military University of Technology, Warsaw, Poland, in 2009, 2011, and 2021, respectively. He is currently an Assistant Professor and the Deputy Director of the Institute of Communications Systems of the Faculty of Electronics, Military University of Technology. His research focuses on digital signal processing, wireless communications, modelling and measurements of radio channels, and localization techniques.

Jan M. Kelner (Member, IEEE) received his M.Sc. degree (Hons.) in applied physics, a Ph.D. degree in telecommunications, and a MBA degree in cybersecurity management from the Military University of Technology (WAT), Warsaw, Poland, in 2001, 2011, and 2024, respectively, and the D.Sc. (habilitation) degree in information and communication technology from the AGH University of Science and Technology, Krakow, Poland, in 2020. He is currently an Associate Professor with the Institute of Communications Systems, Faculty of Electronics, WAT, where he started work in 2003. From 2021 to 2024, he was the Institute Director. Since September 2024, he has been the Faculty Dean. From 2017 to 2024, he was a Principal Voting Member of the Information Systems Technology Panel Operating within the NATO Science and Technology Organisation. He has been an Expert with the European Defence Agency (EDA) CapTech Information and the Office of Electronic Communications, since 2019 and 2022, respectively. Since 2001, he has been involved in many research and development projects for the Ministry of National Defence, EDA, the National Centre for Research and Development, and the National Science Centre. He is also the Manager of four research projects and the Supervisor for twelve Ph.D. students. He has authored or co-authored more than 270 articles in peer-reviewed journals and conferences. He is a reviewer for 35 scientific journals and about 20 conferences. His current research interests include wireless communications, modelling and measurements of radio channels, quality of services in mobile networks, electronic warfare, localization techniques, counter-unmanned aircraft systems.

Cezary Ziółkowski was born in Poland, in 1954. He received the M.Sc. degree in telecommunications engineering from the Military University of *Technolog*y (WAT), Warsaw, Poland, in 1978, the M.Sc. degree in mathematics (specialty–applied mathematical analysis) from the University of Warsaw, in 1989, and the Ph.D. degree in telecommunications engineering and the D.Sc. (habilitation) degree in radio communications from WAT, in 1993 and 2013, respectively. From 1982 to 2013, he was a researcher and a lecturer with the Faculty of Electronics, WAT, where he has been an Associate Professor since 2013. He was engaged in many research projects, especially in the fields of radio communications systems engineering, radio wave propagations, radio communication network resources management, and electromagnetic compatibility in radio communication systems. He is the author or the co-author of more than 200 scientific articles and research reports.

Czesław Leśnik received his M.Sc. (E.E.) degree in electronics and the Ph.D. and D.Sc. degrees in telecommunications from the Military University of Technology (WAT), Warsaw, Poland, in 1978, 1999, and 2018, respectively. Since 1981, he has been employed with the Institute of Radioelectronics, Faculty of Electronics, WAT, where he has been an Associate Professor since 2018. His professional activity focuses on radar theory and techniques, and signal processing.